Systematic Scientific Journal
ISSN: 2675-521

ALKALI-ACTIVATION OF METAKAOLIN AND BRICK RESIDUE GROUND WITH SODIUM HYDROXIDE: INFLUENCE OF MOLARITY AND CURING TEMPERATURE

https://doi.org/10.56238/rcsv15n2-008

Submitted on: 01/19/2025 **Approval date**: 02/19/2025

R.C. Novaes-Rangel[1], D.P. Dias[2] and J.C. Soares[3]

ABSTRACT

Alkali-activated cements are construction materials that have historical origins linked to the 1940s, when they were explored as an alternative to Portland cement. Over the decades, research in this area has progressed, making them an innovative and sustainable option in civil construction, with properties that favor durability and resistance. In this study, the mortar with 100% metakaolin (MC) as a precursor reached maximum compressive strength (34.5 MPa) when activated at 12.5 mol/liter and cured at 80ºC. However, as the ground brick residue (RTM) was added, the peak compressive strength shifted to mortars with lower molar concentrations of the alkaline activator. The lowest resistance was 0.4 MPa in the sample with 100% RTM, activated with 12.5 mol/liter and cured at room temperature. This difference of 86.5 times has several causes, including the degree of crystallinity of the RTM, the high viscosity of the mixture, which made compaction difficult, and the gradual loss of water due to the non-formation of a compact matrix. In the capillary water absorption test, mortars with 100% RTM showed efflorescence, evidencing the low technical feasibility for its use. This study demonstrated the superiority of CM over RTM and the significant strength gain of these mortars when subjected to thermal curing. It was observed that the curing temperature for low molarities did not statistically influence the compressive strength. However, this factor was preponderant in the amount of efflorescence formed.

Keywords: Alkaline Activation. Metakaolin. Ground Brick Residue. Efflorescence.

[1] Universidade Estadual do Norte Fluminense - UENF, Laboratory of Civil Engineering, Campos dos Goytacazes, Brazil.
E-mail: renancnr@gmail.com
ORCID: https://orcid.org/0000-0002-1155-0062
[2] Universidade Estadual do Norte Fluminense - UENF, Laboratory of Civil Engineering, Campos dos Goytacazes, Brazil.
ORCID: https://orcid.org/0000-0003-1645-1538
[3] Instituto Federal Fluminense - IFF, Campos dos Goytacazes, Brazil.
ORCID: https://orcid.org/0000-0002-8474-3877

Systematic Scientific Journal
ISSN: 2675-521

INTRODUCTION

The cement industry is an important source of carbon dioxide (CO2) emissions, contributing significantly to the increase in the levels of this greenhouse gas in the atmosphere [1]. The production of clinker, the main component of cement, involves the decarbonation of limestone, releasing CO2 as a byproduct. These emissions, together with the burning of fossil fuels in the production phase, exacerbate the environmental impact [2]. It is estimated that the concrete industry will produce by the year 2050 about 5.5 billion tons of carbon dioxide [3]. Consequently, there is an abundance of research aimed at partially or totally replacing Portland cement in civil construction. Alkali-activated cements stand out as one of the most promising alternatives for this substitution [4].

Studies of these materials described by Purdon in the 1940s were the first to obtain as a result gains in mechanical strength in compounds based on blast furnace slag and sodium hydroxide, which are considered one of the milestones in this line of research. The contributions to the field of alkali-activated materials were intensifying, until in 1967 Glukhovsky engaged in the development of materials based on aluminosilicate solutions with low or no calcium and alkali metal content, calling them cement-soils and silicate soils [5].

Glukhovsky observed two groups of materials, the low-calcium system and the high-calcium *system* [6]. It was observed that the products of the first group had 3D-polymeric structures, being similar to natural zeolites, micas and feldspathoids. The types of products formed by alkali-activation of precursors depend on the curing conditions, nature of the alkaline activator and the precursors used, among other parameters [7].

The *low calcium* system [6], which was used in the present work, originates from the $(Na,K)_{2O-Al2O3}$ – SiO2 – H2O model. The product formed is an amorphous matrix with agglomerating properties, whose main component is an aluminosilicate gel known as N-A-S-H or zeolitic precursor [8].

Davidovits' studies in the 1940s are considered another milestone in this line of research, but it was with the advent of new technologies that it was possible to understand the molecular interaction of alkali-activation products [8, 9, 10].

Nuclear magnetic resonance (NMR) studies have shown that, at the nanoscopic scale, the gel resulting from alkali-activation has a three-dimensional structure, in which Si is found in different forms, with a predominance of the Q4(3Al) and Q4(2Al) units. Different types of zeolites (hydroxysodalite, Na-chabazite, zeolite P, and so on) are usually obtained as products of secondary reactions [11, 12].

Systematic Scientific Journal
ISSN: 2675-521

The dissolution of siloxane (Si–O–Si) in silanol (–Si–OH) and/or sialate (–Si–O–) in an alkaline medium forms Si–O–R+ (being R ion of Family 1A of the Periodic Table). The agglomeration of these monomers forms dimers (Si-O-Si bonds) catalyzed by hydroxyls OH^-. The clusters formed from the polymerization of $(HO^-)_{3}Si–OH$ grow and expand, generating colloids. Nevertheless, the aluminum of $Al(OH)^{-4}$, originated in the first stage of activation, isomorphically replaces the silicon in the formed tetrahedron. While the alkali metal catalyzes the reaction in the first stage, in the second it acts as a structural component [9, 11, 12].

In the present work, ground brick residue (RTM) and metakaolin (MC) were used as precursors in systems activated with sodium hydroxide, in order to establish comparative standards between them.

The use of ground brick waste in civil construction has stood out as a sustainable and efficient practice. By incorporating this waste into construction processes, not only is improper disposal avoided, but several areas are also benefited. Ground brick can be used in the production of mortars, concrete, and blocks, providing greater mechanical strength and reducing the demand for natural resources.

This approach directly contributes to reducing environmental impact, promoting the circular economy in construction. Additionally, utilizing brick waste can result in lower costs, making it an economically advantageous alternative. This practice is in line with the principles of sustainability in civil construction, demonstrating that it is possible to promote efficiency and environmental responsibility without compromising the quality of built structures.

The use of RTM activated with sodium hydroxide in this research has a doubly ecological bias: firstly, the total or partial replacement of metakaolin, and secondly, the replacement of a natural raw material by an industrial waste in the production of binders, as well as offering an alternative to Portland cement in civil construction.

The other precursor used, MC, is well known in the field of alkali-activated materials [1, 8, 12], but the lack of studies of alkaline activation only with sodium hydroxide in wide ranges of alkaline activator molarity was identified and, therefore, explored in this work. The use of sodium hydroxide as an alkaline activator offers advantages over the use of potassium hydroxide, due to the lower cost and greater availability of the product.

The formation of efflorescence has already been described in several studies on sodium hydroxide activation. This study allows a broader view of the subject, as it uses different molar concentrations, precursors and curing temperatures.

Systematic Scientific Journal
ISSN: 2675-521

MATERIALS AND METHODS

Ground brick residue, metakaolin, sand and alkaline NaOH activator solution were used to make the mortars.

The brick residue was dried in an oven at 100°C for 24 hours and then ground in 4 kg batches for 1 hour in a ball mill. The evaluation of grinding time *versus* fineness of the RTM was well discussed by [13], and grinding times longer than one hour did not lead to a significant decrease in particle size.

The® HP ultra metakaolin from Metacaulim do Brasil S/A, sold in 20 kg bags, was used as the second precursor (reference). The chemical composition and physical characteristics are shown in Table 1.

Table 1 - Physical and chemical characteristics of the precursors.

	Al2O3	SiO2	Fe2O3	SO3	TiO2	K2O	MnO	Dog	Other	*g/cm3	**D50 (mm)
MC	46,75	44,02	4,86	1,43	1,36	1,21	0,13	0,00	0,23	2,57	0,015
RTM	36,98	47,61	9,30	1,47	1,51	1,51	0,07	0,61	0,17	2,75	0,008

* apparent specific mass of the precursors.
** Average particle diameter of precursors.

The X-ray diffraction assay (XRD) was adopted to identify crystalline phases in the RTM and MC, using a Miniflex 600 diffractometer of the Rigaku brand, with a voltage of 40 kV, 15mA, Cu-Kα radiation with a step of 2θ = 0.02° and a scanning speed of 10°/minute, for the range of 8 to 70°. Figure 1 shows the results obtained in the XRD analyses.

Analyzing the XRD result (Figure 1), a diffuse halo characteristic of non-crystalline materials (amorphous) is observed in the CM sample, indicating an amorphous characteristic of this material, as described by [14]. The 2θ broadband between 16 and 38° indicates the presence of material with short-range atomic ordering. Thus, the identified amorphous aluminosilicates are extremely important for the production of geopolymers, due to their high dissolution rate in a highly alkaline environment [15].

Figure 1 - XRD of the precursors.

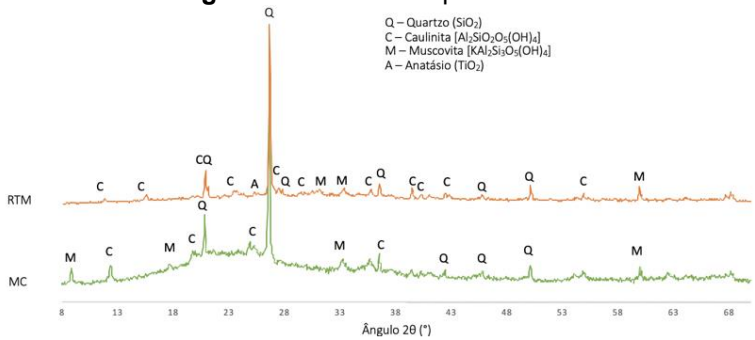

Systematic Scientific Journal
ISSN: 2675-521

Figure 1 shows that the MC, between 11 and 45º, has a very pronounced amorphous halo. The same behavior is not seen in RTM, suggesting the presence of crystalline or poorly amorphous material. In view of this, it can be said that metakaolin is more vitreous than ground brick waste, i.e., the former is a better precursor for the manufacture of alkali-activated cements (CAT) than the latter, due to the probable greater reactivity.

In the preparation of the alkaline activator solutions, commercial sodium hydroxide in scales with a purity equal to 75.2% was used, in addition to water from the public network, which was previously distilled in a Quimis Q341-210 equipment.

Normal sand [16] supplied by the Institute of Technological Research of the State of São Paulo (IPT/SP) was used. Equal portions of four commercial fractions were used: #16, #30, #50 and #100. The apparent specific mass was 2.65 g/cm3, the porosity was 0.85% and the BET specific surface was 0.28 m2/g.

Three different precursors, five molar concentrations of alkaline activating solution and three curing temperatures were studied (Table 2). In all, 45 impressions were made, using a mass ratio of 1:1:0.8 of precursor, fine aggregate and alkaline activating solution, respectively. The mixing process of the components was carried out using an EMIC benchtop planetary mixer, model AG-5, respecting the following sequence: addition of the activator solution to the vat, addition of the precursor and, later, the sand, and the total process lasted 150 seconds. After completing the mixing process, the consistency of the different mortars in the fresh state was evaluated according to the prescriptions of the Brazilian standard [17].

In order to evaluate the effect of the curing temperature on the mechanical strength of the mortars, three temperatures were adopted: ambient, 60°C and 80°C. The curing procedure at temperatures of 60°C and 80°C was carried out in a muffle oven for 24 h ± 30 min and then conditioning at room temperature for 27 days. The ambient temperature was carried out in the laboratory at 27.3 ± °C and relative humidity of 65.5 ± %. All mortars were removed from the molds after 24 hours, with the exception of RTM-100%, which did not acquire sufficient strength in this period, requiring a total of 7 days to perform the demolding.

Systematic Scientific Journal
ISSN: 2675-521

Table 2 - Project variables.

Precursor	Molar concentration (mol/l)	Healing
RTM-100% MC-100% MC+RTM-50%	6,0	Environment 60°C 80°C
	8,0	
	10,0	
	12,5	
	15,0	

In the hardened state, the mortars were evaluated according to their behavior against the phenomenon of efflorescence (visual inspection), resistance to axial compression [17] and water absorption by capillarity [18].

For the axial compression tests of the mortars, cylindrical specimens with dimensions of ∅50 mm x 100 mm were molded, being tested in a Solotest press with a capacity of 1000 kN and a loading speed of 0.3 MPa/s. It was used as a release agent in the 15W-40 mineral oil molds, as described in [17]. Three different graphs were plotted with the values of the axial compressive strengths, according to the precursor used. The analysis of variance was performed in the *Past software*, version 4.07b, and the data entry in the *software* followed the methodology of [14].

To determine the capillarity coefficient and water absorption by capillarity, the Brazilian standard was used [18]. Due to the low availability of raw material for laboratory tests, it was necessary to adopt a specimen model with reduced dimensions. Therefore, cubes with 40 mm edge were used instead of prisms with 40 mm x 40 mm x 160 mm. To segment the prism into three identical cubes, a Cortag electric circular saw, model ZAPP 200, was used. Each cube was sanded (sandpaper no. 100), cleaned and identified. To measure the dimensions of each cube, a caliper was used, and to weigh them a scale with a precision of 0.01 g.

Different analytical techniques were applied in this work, aiming to understand the geopolymerization process, and several proportions were evaluated in alkali-activated pastes. Isothermal calorimetry was applied to study the kinetics of geopolymerization, and was performed in an isothermal calorimeter of Calmetrix, model I-CAL 2000 HPC, with 2 data acquisition channels. It is worth mentioning that, due to the non-reactive nature of the sand, pastes were used instead of mortars in the calorimetric studies. Scanning electron microscopy (SEM) analyses were performed in a Shimadzu Superscan SSX550 equipment, aiming at the study of the microstructure. The images were made in sections by the backscattered electron imaging (*BSE*) mode, working with an acceleration voltage of 15 kV. Finally, the X-ray diffraction analysis allowed the identification of the main crystalline phases formed in the produced mortars.

Systematic Scientific Journal
ISSN: 2675-521

Throughout the present study, due to the high number of mortars, the following nomenclature was used to refer to them: Precursor (RTM or MC) – percentage of precursor in the mixture (100% or 50%) – molar concentration of the activator, in mol/liter (6, 8, 10, 12.5 or 15) – curing condition (A for environment, 60 to 60°C and 80 to 80°C).

RESULTS

FRESH STATE

Consistency (flow table test)

The result of the spreading of the 15 mixtures is shown in Figure 2, a procedure prescribed in the Brazilian standard [19]. The difference between the mortar with the highest and the lowest spreading was 41% (mortar with 100% RTM as the precursor activated with 6 mol/liter and the mortar with 100% MC activated with 15 mol/liter, respectively).

Figure 2 - Slump of the mortar cone trunk in the *flow table test*.

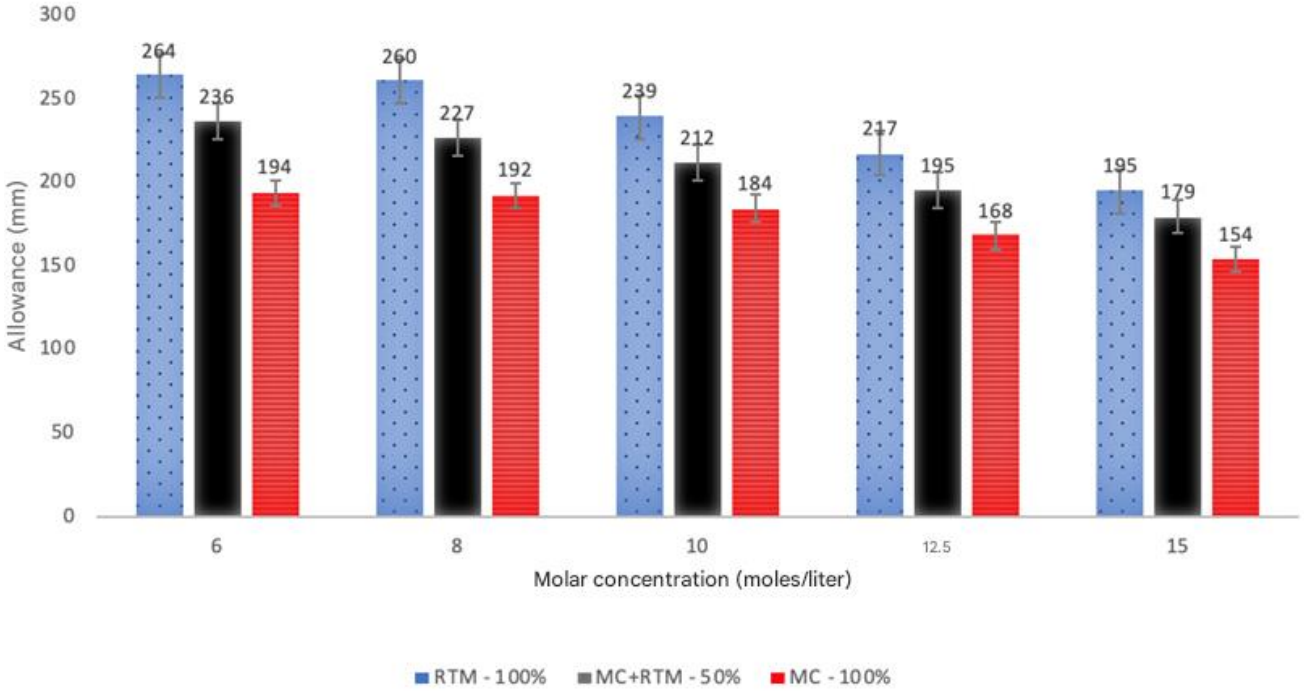

It is verified that the workability of the mortars decreases with the increase of the molar concentration of the alkaline activating solution. It is also noted that for the same molar concentration, the greater the amount of MC, the lower the workability of the mixture. This behavior occurred in all molar concentrations evaluated.

The characteristics of the precursor grains interfere with the workability of the mortars. The mean particle diameter (d50), shown in Table 1, indicates that the ground brick

Systematic Scientific Journal
ISSN: 2675-521

residue is finer than metakaolin, which indicates a higher water demand of the former in relation to the latter precursor. The surface area has a great influence on the workability of mortars. High specific surfaces indicate high partial absorption of liquid, decreasing the free water in the system due to the wall effect and, consequently, making the mixture less fluid.

Mortars with 50% metakaolin and 50% ground brick residue (MC+RTM-50%) have intermediate abatement values in relation to those with 100%, i.e., the rule of mixtures and proportions is verified.

According to the classification of [19], the consistency index of RTM-100% mortars is high (above 250 mm) to very high (180 mm - 250 mm). MC+RTM-50% and MC-100% mortars are classified as high (above 250 mm) to moderate (150 mm - 180 mm).

HARDENED STATE

Qualitative visual analysis

Figure 3 shows the specimens of all mortars. Observing these images, the presence of efflorescence in all the specimens can be noted.

Efflorescence is the phenomenon in which the sodium present in the matrix is carried to the external environment due to its solubility in water and the presence of microcracks in the material. The density of the matrix and the concentration of this chemical element in the activating solutions influence the occurrence of this phenomenon. According to [20], when ions undergo hydration, several water molecules are formed by electrical attraction, and a sphere around the ion, called a hydration sphere, is formed. [21]. They consider that the efflorescence in geopolymers based on sodium hydroxide as an activating solution occurs due to the weak chemical bond of Na+ to the structure of the geopolymers and the high mobility of the Na+ cation.

Efflorescence occurs by the migration of sodium from the interior of the matrix, which is soluble in water, to the surface of the sample. Efflorescence is therefore dependent on the microstructural characteristics of the geopolymers and is influenced by the humidity and temperature of the environment [22].

Research [20] reported that alkali-activated metakaolin mortars with NaOH exhibited exudation, efflorescence, and carbonation. They attributed this behavior to the atomic radius and the high solubility of Na+.

The influence of dosage on efflorescence formation in metakaolin geopolymers were also studied [22]. The chemical composition of the precursor and the molarity range of the alkaline activator were different from those used in the present study; however, intense

Systematic Scientific Journal
ISSN: 2675-521

efflorescence formation was also identified in the specimens. Therefore, it is inferred that efflorescence formation seems to be more linked to the nature of the alkaline activator (NaOH) than to the quality of the precursor.

Figure 3 - Activated mortars with five concentrations: 6, 8, 10, 12.5 and 15 mol/liter, from left to right, respectively. (a) MC-100% cured at room temperature. (b) MC-100% cured at 60ºC. (c) MC-100% cured at 80ºC. (d) RTM-100% cured at room temperature. (e) RTM-100% cured at 60ºC. (f) RTM-100% cured at 80ºC. (g) MC+RTM-50% cured at room temperature. (h) MC+RTM-50% cured at 60ºC. (i) MC+RTM-50% cured at 80ºC.

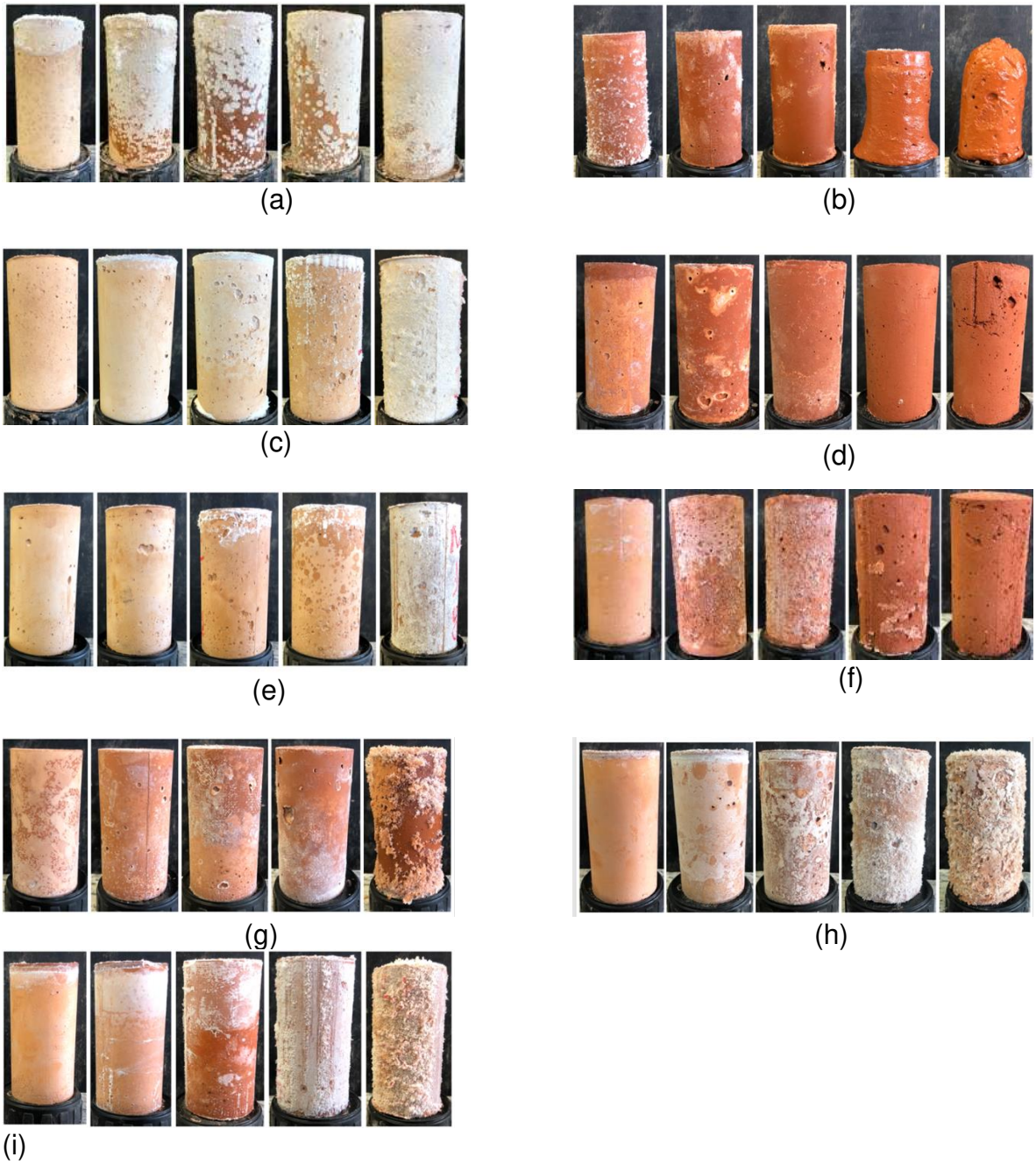

Systematic Scientific Journal
ISSN: 2675-521

Axial Compressive Strength

Figure 4 shows the axial compressive strength of mortars tested at 28 days with 100% metakaolin as a precursor. The results indicate that at 6 mol/liter the molar concentration of the alkaline activator was not sufficient to promote the destructuring of the precursor. However, as the molar concentration increased, the mechanical strength also increased, up to the maximum value at 12.5 mol/liter. The drop in resistance evidenced in mixtures with a molar concentration of 15 mol/liter may be related to the high viscosity of the alkaline solution and, consequently, to the low workability of the mixture, which hindered the process of densification of the specimens. In addition, it is noted that thermal curing caused a gradual increase in compressive strength in mortars with molar concentrations of 6, 8, 10 and 12.5 mol/liter.

It can be noted that mortars activated with 15 mol/liter had a marked decrease in mechanical resistance, around 57%. This event may be associated with thermal stresses and water loss due to drying. Thermal stresses caused microcracks in the matrix, reducing the resistance to axial compression. In addition to this effect, drying, intensified by thermal curing, decreased water needed for the destructuring and recombination of the precursor, leading to low mechanical performance.

Tukey's test [23] was the statistical method used to compare the results obtained and identify significant differences, contributing to the analysis and interpretation of the data. Thus, it was possible to conclude that in the dosages with 100% MC there is no significant difference between the mortars activated with 6 mol/liter (room cure, 60°C and 80°C) and with 8 mol/liter (room cure). In addition, it was also evident that the MC-100%-15-A mortar does not differ from the MC-100%-12.5-60 and the MC-100%-12.5-80. Based on these results, it was decided to conduct subsequent assays with 100% activated MC-assays with molar concentrations of 8, 10 and 12.5 mol/liter.

Figure 4 - Axial compressive strength of MC-100% mortars.

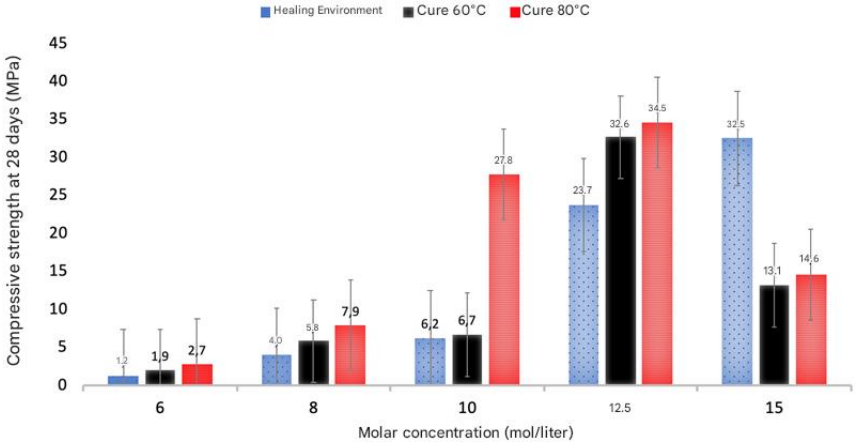

Systematic Scientific Journal
ISSN: 2675-521

Figure 5 shows the result of axial compression of mortars with 50% metakaolin and 50% RTM as precursor. It can be observed that, for these proportions, there is a displacement of the highest mechanical resistance for mortars with molar concentrations of 8 and 10 mol/liter, especially at curing temperatures at 80°C. In addition, at 6 and 15 mol/liter the lowest resistances are observed, and this behavior is related to different reasons. At 6 mol/liter, the low alkalinity of the medium was not able to destructure the precursor, as suggested [24]. At 15 mol/liter, the high viscosity or low workability may have impaired the compaction of the specimens and, consequently, increased the porosity of the matrix.

The increase in the curing temperature had a beneficial effect on mortars with molar concentrations of 8 and 10 mol/liter. At 12.5 and 15 mol/liter there was a decrease in resistance, but within the margins of error. Thus, this behavior is possibly related to the combined effect between the viscosity of the alkaline activating solution, which prevents efficient alkali-activation, and the accelerated loss of water due to the increase in temperature.

The mortars MC+RTM-50%-6-A and MC+RTM-50%-6-60 were the ones that presented the lowest compressive strengths, reaching 2.0 MPa. This value corresponds to 18.9% of the highest mechanical strength of the MC+RTM-50%-8-80 mortar (10.6 MPa).

Figure 5 - Axial compressive strength of MC+RTM-50% mortars.

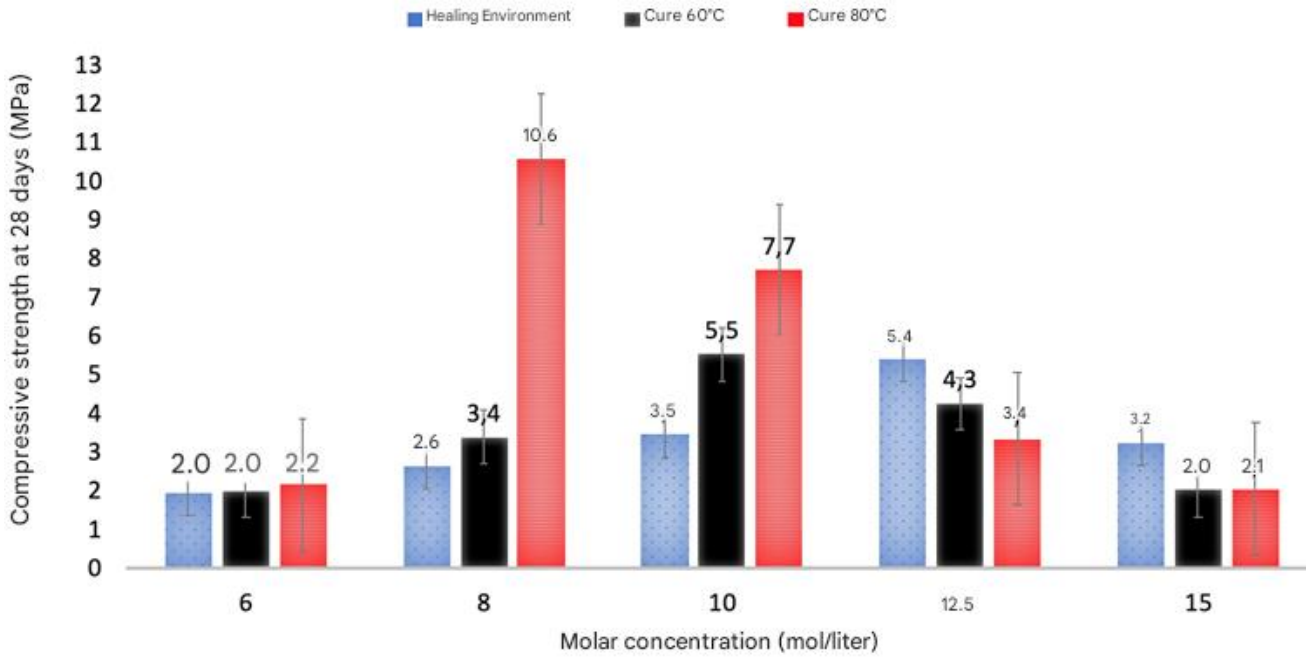

Figure 6 shows the axial compressive strength of the mortar specimens with 100% RTM as a precursor. Following the trend of shifting the peak resistance to lower molar

Systematic Scientific Journal
ISSN: 2675-521

concentrations, with the complete replacement of MC by RTM, the peak was shifted to 6 mol/liter. It is also observed that, at higher molar concentrations, the resistance of the specimens dropped drastically, so that the RTM-100%-12.5-A, RTM-100%-15-60 and RTM-100%-15-80 dosages could not be measured, because the mortars did not harden.

Figure 6 - Axial compressive strength of RTM-100% mortars.

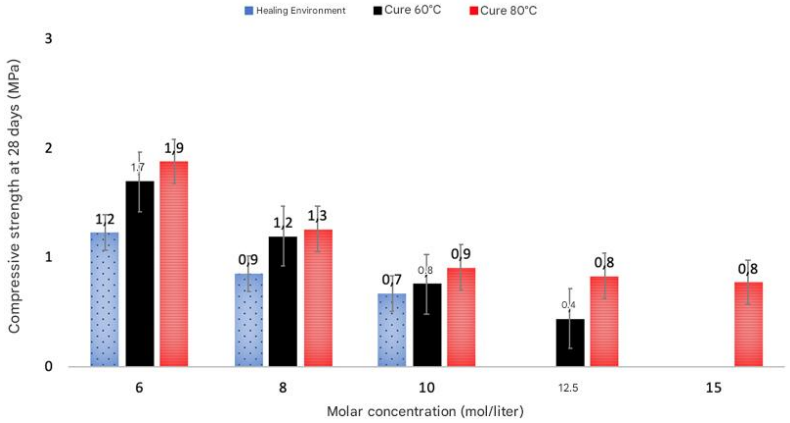

The increase in temperature positively influenced the mechanical strength of the mortars, even allowing the rupture of those with higher molar concentrations of alkaline activator that could not be demolded when cured at room temperature.

Among all the mortars produced, the most resistant was MC-100%-12.5-80, which reached 34.5 MPa. This value represents 86.5 times the lowest strength (0.4 MPa), which was of the RTM-100%-12.5-60 mortar. In addition, it is worth mentioning that the alkaline activating solution in both mortars was 12.5 mol/liter of NaOH.

When comparing the axial compressive strength (Figures 4 to 6) with the qualitative visual analysis, it is observed that the dosages with MC-100% and MC+RTM-50% showed that higher amounts of alkaline activator resulted in greater efflorescence formation. However, the dosage with 100% RTM-as a precursor showed greater efflorescence formation and higher compressive strengths at lower molar concentrations. The low reactivity of RTM may explain this behavior (Figure 1), because at higher molar concentrations of alkaline activator, a totally solid state was not obtained, which prevented the migration of NaOH crystals through the microcracks and pores in the hardened state.

Regarding the statistical analysis by Tukey's method [23], in mortars with RTM-100% the compressive strength did not present a significant difference between RTM-100%-10-80, RTM-100%-12.5-80 and RTM-100%-15-80. Thus, the first mortar was chosen to carry out the subsequent tests. In addition, it was also decided to evaluate the mortar with 6 mol/liter, since it presented the greatest significant differences in relation to the others.

Systematic Scientific Journal
ISSN: 2675-521

Although Tukey's test was used in the analysis of the results of the axial compressive strength of MC+RTM-50% mortars, its conclusions will not be discussed, because as already mentioned, the rule of mixtures could be verified and the values will be intermediate to MC-100% and RTM-100%. In this way, it was possible to reduce the amounts of data under analysis and direct the conclusions in what was defined as the objective of this work.

It is essential to note, then, that the tests discussed from now on only contemplated those of MC-100% and RTM-100% mortars, which presented significant differences. This methodology was applied in order to reduce the amount of data and techniques used to reach adequate conclusions.

Water absorption by capillary

Table 3 shows the water absorption by capillarity in 10 minutes (A10) and 90 minutes (A90), in addition to the capillarity coefficient (C) of mortars with 100% metakaolin. It can be noted that for the same type of cure, both the water absorption by capillarity and the capillarity coefficient decrease with increasing molarity of the activating solution. The two curing environments provided relatively similar results, with the exception of MC-100%-15-80, which has values very close to those of the mortar with molar concentration equal to 12.5 mol/liter.

[25] reached saturation in NaOH and KOH-activated metakaolin geopolymers when cured at 50°C between 60 minutes and 90 minutes. Capillary absorption was around 2.5 g/cm2 and did not differ significantly. In the present study, at 60 minutes of the test, the mortars MC-100%-8-A, MC-100%-8-80, MC-100%-10-A, MC-100%-10-80 reached saturation. The mortars with the highest molar concentration of alkaline activator (Figures 7 and 8) reached saturation around 270 minutes. It is worth mentioning that the mortars activated with 12.5 and 15 mol/liter absorbed by capillarity, at 90 minutes, about 19% of the water in relation to the mortars that were activated with 8 and 10 mol/liter.

Table 3 - Results of the capillary water absorption test, according to NBR 15259 [18].

Precursor	Healing	mol/l	A10 (g/cm2)	A9 (g/cm2)	C $(d/dm2)^{1/2}$
MC-100%	Environment	8,0	0,52	1,05	16,88
		10,0	0,34	0,85	13,58
		12,5	0,06	0,20	3,17
		15,0	0,00	0,01	0,20
	80°C	8,0	0,75	1,10	17,59
		10,0	0,34	0,78	12,43
		12,5	0,07	0,20	3,19
		15,0	0,07	0,22	0,47

Systematic Scientific Journal
ISSN: 2675-521

[26] and [27] emphasize that capillary absorption is one of the main mechanisms of transport and entry of aggressive agents into the pores of mortars and, therefore, is of great importance for the durability of the structures. Thus, water absorption by capillarity is also related to efflorescence formation, so both parameters must be analyzed together. Wetting and drying cycles tend to carry NaOH, which is soluble in water, to the outside of the matrix more intensely. This mechanism can bring damage and endanger the integrity of the material in the long run.

Figure 7 - Absorbed water mass *versus* time curves for mortars with 100% metakaolin cured at room temperature.

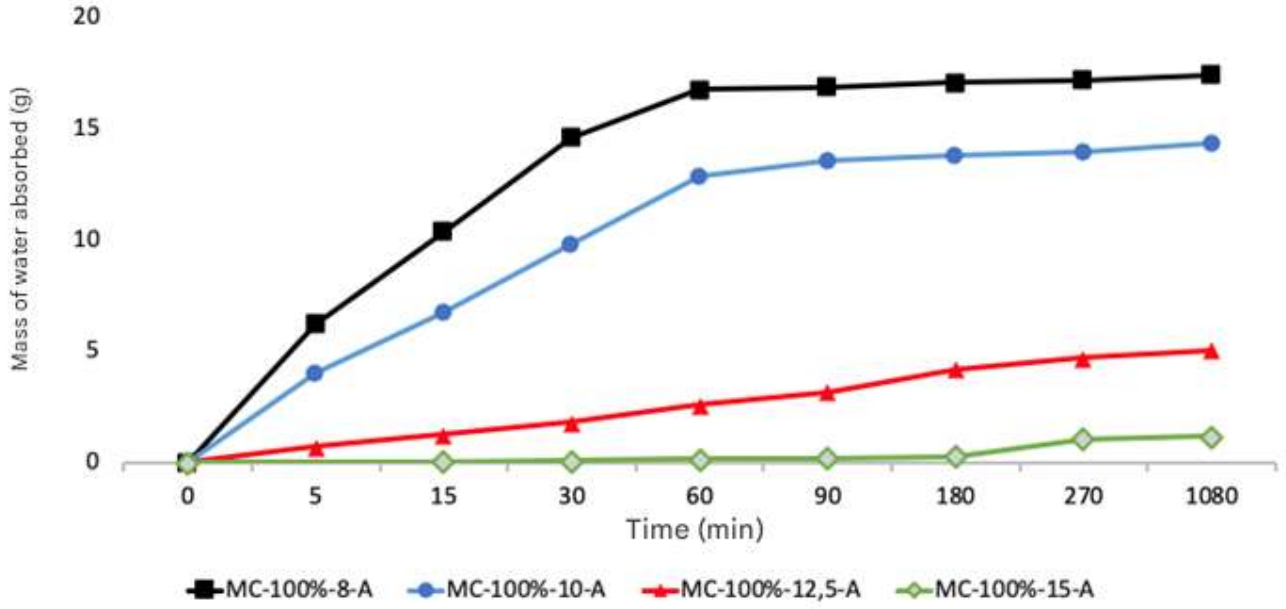

Figure 8 - Absorbed water mass *versus* time curves for mortars with 100% metakaolin cured at 80ºC.

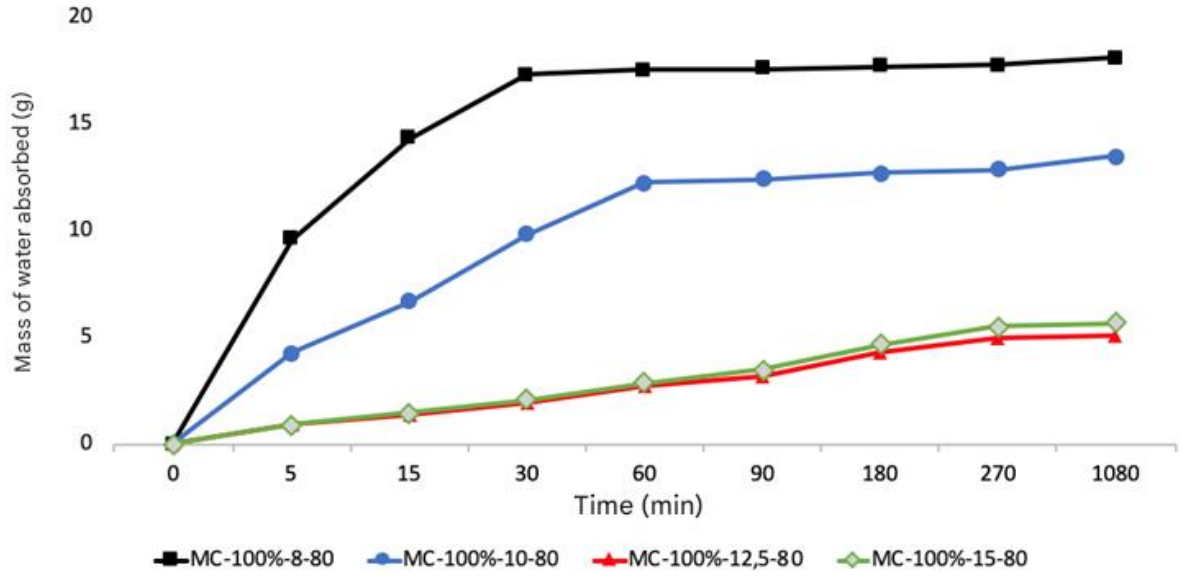

Systematic Scientific Journal
ISSN: 2675-521

According to Table 4, the mortars were classified as C6, C4 or C1. It is worth mentioning that the test model was adapted, not following all the prescriptions of the Brazilian technical standards [18, 28]. However, a satisfactory approximation could be made, due to the similarities between the methods used, either by dosage or by test method, and, therefore, the comparison of the results obtained in the present study with others in the literature is inconsistent.

Table 4 - Classification of mortars according to ABNT NBR 13281 [28].

Mortar	C (g/dm²·min1/2)	Classification
MC-100%-8-A	16,88	C6
MC-100%-8-80	17,59	C6
MC-100%-10-A	13,58	C6
MC-100%-10-80	12,43	C6
MC-100%-12.5-A	3,17	C4
MC-100%-12.5-80	3,19	C4
MC-100%-15-A	0,20	C1
MC-100%-15-80	0,47	C1

According to [29], mortars classified as C6 indicate high permeability. This characteristic is not suitable for coating mortars, as permeability is related to the susceptibility of materials to degradation. A permeable material is more porous, but it is worth mentioning that for the material to be permeable, there needs to be interconnection between the pores.

Mortars with RTM-100%, both at room curing and at 80°C, showed mass loss when immersed in water. Part of the mortar was carried by the water. This loss of mass was caused by the disaggregation of the mortar in the liquid medium (Figure 9). This behavior caused imprecision in the values of capillarity coefficient and water absorption by capillarity. It is worth noting that the highest mass losses were observed in mortars with lower axial compressive strengths. This behavior was associated with the low resistance of the mortars and the leaching of their constituents. This behavior is shown in Figure 7.

Figure 9 - Loss of mass of RTM-based mortars.

Systematic Scientific Journal
ISSN: 2675-521

ANALYTICAL TECHNIQUES

Calorimetric study

After the analysis of the results of the physical and mechanical properties, four alkali-activated pastes were analyzed using the isothermal calorimetry technique, namely: MC-100%-8, MC-100%-12.5, RTM-100%-6 and RTM-100%-10. It should be noted that the assay time of the metakaolin-based samples (2 days) was different from the samples with ground brick residue (7 days), since the latter required more time for demolding.

Figure 10 shows the heat flux of the MC-100%-8 and MC-100%-12.5 pastes in a controlled environment at 23°C for 48 hours. It is noted that the peak is reached after 12 minutes of testing and that up to two hours there is an increase in the thermal energy released with the increase in the concentration of the activating solution.

Figure 10 - Heat flux of the MC-100%-8 and MC-100%-12.5 pastes.

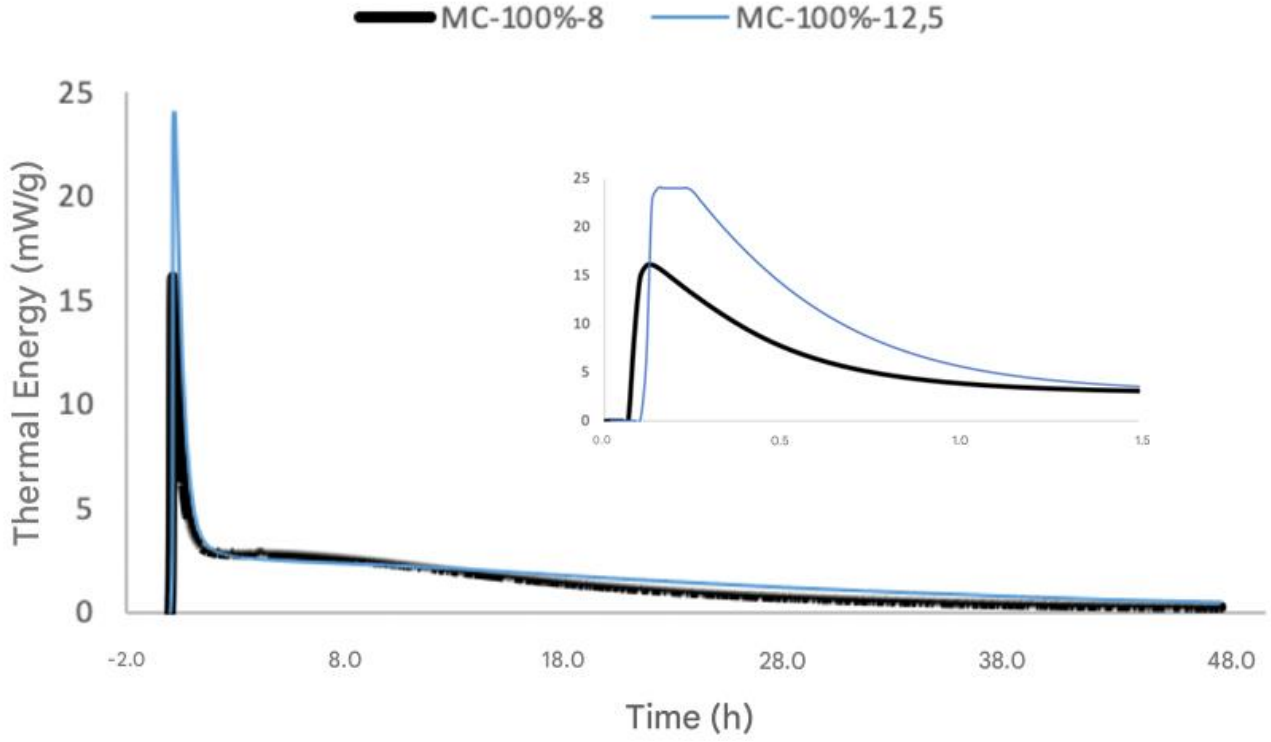

The gain in mechanical strength in alkali-activated pastes is due to geopolymerization reactions, because in the first hours the siloxane (Si–O–Si) bonds are broken into silanol (–Si–OH) and/or sialate (–Si–O–) and are catalyzed by the hydroxyls OH^- of the alkaline activator. At first, there is an intense exothermic reaction, observed at the peak in 12 minutes after the mixing of the raw materials. As the molarity of the alkaline activator increases, the greater the amount of OH^- hydroxyls available, destabilizing the siloxane bonds and increasing the heat released [30].

Systematic Scientific Journal
ISSN: 2675-521

According to [24], clusters of monomers and dimers are generated in polymerization, forming tetrahedra of (HO-)$_{3Si–OH}$ that grow, expand and generate colloids. Aluminum is also responsible for part of the energy released, as the Al–O–Si bonds are broken and bond to the hydroxyls, forming $Al(OH)^{-4}$.

This behavior explains the significant difference between the thermal energy values of the MC-100%-12.5 (25 mW/g) and MC-100%-8 (18 mW/g) paste at 12 minutes, as well as the values of mechanical resistance in ambient curing at 28 days (Figure 4). This behavior was also observed by [31].

In the RTM-based folders (Figure 11) it is observed that the curves are similar, almost overlapping. The peak thermal energy released in both samples was approximately 8 mW/g for a time equal to 6 minutes after mixing. In addition, it is noted that the paste with the lowest molar concentration of alkaline activator released a little more energy. This result is associated with the greater formation of stable products, since mortars with this molar concentration also achieved higher axial compressive strength in relation to mortar with 10 mol/liter. This analysis of the correction between paste and mortar is possible due to the non-reactive nature and chemical stability of the sand.

Figure 11 - Heat flux of the RTM-100%-6 and RTM-100%-10 pastes.

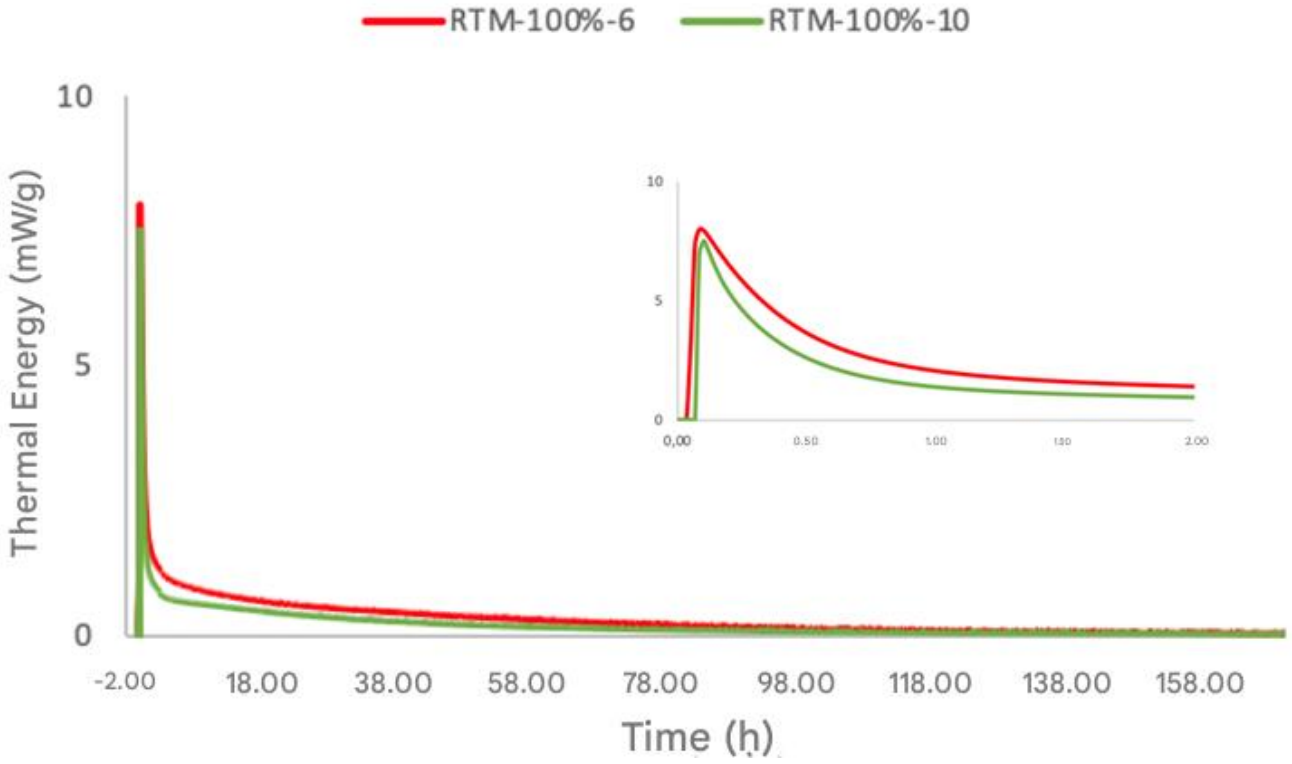

With the increase in the formation of stable products, ionic mobility decreases, as the water is lost by drying or is immobilized inside the matrix. The decrease in the thermal energy released, observed in Figures 10 and 11, corroborates these statements, since after

Systematic Scientific Journal
ISSN: 2675-521

24 hours the values are considerably lower. The development of resistance at an early age is in accordance with the work of [14, 30, 32, 33].

Analyzing the higher axial compressive strengths for low molarities of the activator solution in mortars with RTM (Figure 6), the small amorphous band seen in the XRD of the RTM (Figure 1) and the low heat flux of the mortars (Figure 11) it can be concluded that this precursor has crystalline characteristics and that the molarity of the alkaline activator is not sufficient to break the strong bonds of the precursor constituents. Thus, a large part of the precursor remains inert, contributing to the accentuated leaching observed in the capillary water absorption assay.

When the pastes with different precursors (MC and RTM) are compared, a significant difference in the reaction heat in absolute values is observed. Analyzing the heat of reaction at the end of each of the assays, the RTM-100%-6 paste releases 32% less heat of reaction than the MC-100%-12.5. When analyzing these same samples in a time equal to 48 hours, it can be noticed that the RTM-100%-6 paste releases 72% less heat than the MC-100%-12.5. These values are consistent with the propositions made previously.

Scanning electron microscopy (SEM)

Samples were taken from the interior of the specimens, in the central region, both in height and diameter. It is worth noting that the samples were not from the fracture region of the specimens. These areas showed no signs of visible efflorescence at the time of sample extraction.

It can be highlighted that the time between the preparation of the samples and the performance of the tests may have had a dominant effect on micrographs, especially the presence of efflorescences. In this work, due to problems with equipment, the time was long, favoring the migration of Na+ ions to the surface of the samples.

Figure 12 shows the micrographs of the MC-100%-8-A and RTM-100%-6-80 mortars with a 500x magnification. It is observed that there is the deposition of a layer on the surface of the sample, possibly efflorescence. As previously discussed, alkali-activated mortars with sodium hydroxide usually present this phenomenon when there is an imbalance between the constituent materials.

In a similar increase, [14, 20, 34] reported the presence of homogeneous, porous matrices with cracks and a well-defined small matrix-aggregate interface. However, due to the presence of a high amount of efflorescence, the present study did not present these characteristics. Unlike [20, 21], the only alkaline activator used here was NaOH, while those

Systematic Scientific Journal
ISSN: 2675-521

used sodium silicate or combinations of it with sodium hydroxide. Therefore, the type of alkaline activator is extremely important for the formation or not of efflorescence.

The compact matrix of N-A-S-H (Figure 12) shown in (a) and (e) is the phase responsible for the strength of the alkali-activated mortar. N-A-S-H forms large dense and resistant networks and is related to the breakdown of the molecular structure of the precursor by the action of the alkaline activator. The aggregate grain can be noted in (c) and the abundance of efflorescence formed in (b) and (d).

Figure 12 - (a) MC-100%-8-A mortar; (b) RTM-100%-6-80 mortar (both with 500x magnification).

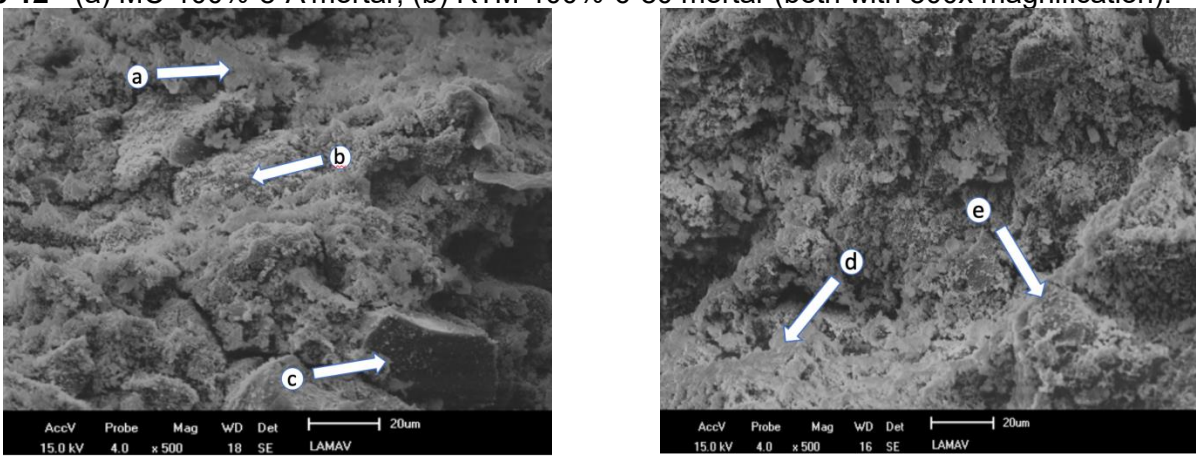

(a) (b)

For an increase equal to 2000x, elongated structures in the shape of needles (acicular morphology) in the form of skeins, possibly efflorescence, could be seen in the MC-100%-12.5-A sample (Figure 13). Such structures have also been observed by [35]. However, only in a localized way. Figure 13a shows a part of the small aggregate. In addition, compact matrix lamellae are also noted (Figure 13b), as described by [36].

Molecular reorganization involves the ability of the alkaline activator to destabilize the precursor. In the micrographs of the mortars with 100% RTM, several unreacted grains were identified (points 2 and 4) and a high rate of efflorescence formation (points 1 and 3). This behavior revealed the activator's inability to break down the RTM structure to form new phases. Thus, in addition to the NaOH being free, the compressive strength is low when compared to mortars with metakaolin.

The micrographs corroborate the results obtained in the calorimetry tests (reaction heat curves), because mortars with a higher amount of unreacted grains, in the case of RTM, have lower reaction heat intensity. Because the reaction for the formation of N-A-S-H is exothermic, fewer reacted grains lead to less heat release.

Systematic Scientific Journal
ISSN: 2675-521

Figure 13 - (a) MC-100%-8-A mortar; (b) RTM-100%-6-80 mortar (both with 2000x magnification).

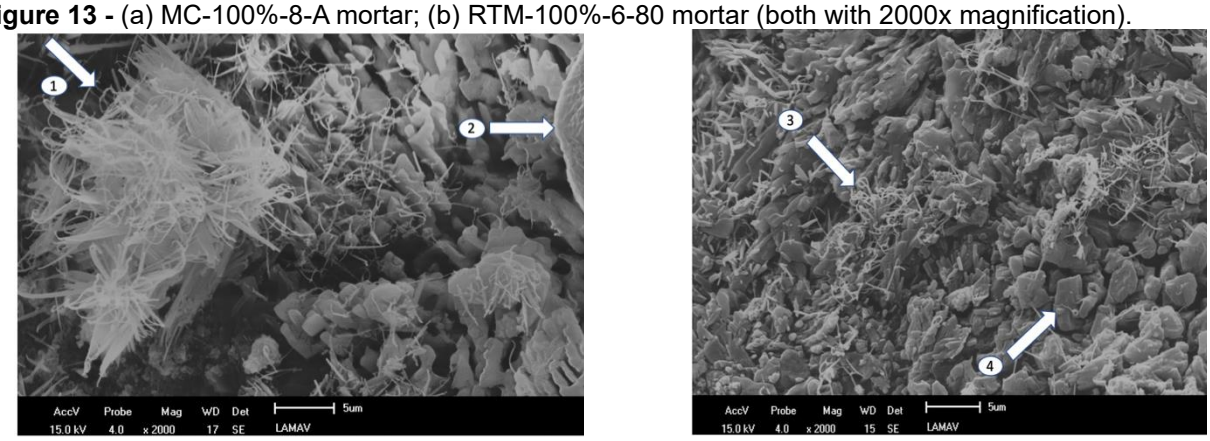

(a) (b)

X-ray Diffraction (XRD)

The main crystalline phases found in XRD were quartz (SiO2), kaolinite ($Al2Si2O5(OH)_4$), muscovite [$KAl2Si3O5(OH)_4$], and anatase (TiO2), as shown in Figure 14.

Regarding the bands of amorphous halos, the analysis of samples submitted to the same type of cure was initially carried out. It was observed that in the sample with the lowest molar concentration of activating solution (MC-100%-8-A), the halo is between 16 and 38°. This angle gradually increases with the increase in the molarity of the activating solution (up to 15 mol/liter).

In samples cured at 80°C, the intensity of the amorphous halo is higher when compared to mortars submitted to ambient curing. In addition, it is also noticed in this group that the final portion of this halo occurs at approximately 44°. This displacement of the amorphous band was also identified by [20, 36], who attributed it to the formation of hydrated aluminosilicate gel (N,K)-A-S-H with random atomic ordering, short-range, rigid and high mechanical strength, formed after contact of metakaolin with the alkaline activating solution.

These results are in agreement with the axial compressive strength (Figure 4), as higher mechanical strength values were found for mortars with higher molar concentrations, thus indicating a higher amount of N-A-S-H formed, since the alkaline activator used in the present study was single-component (NaOH).

Systematic Scientific Journal
ISSN: 2675-521

Figure 14 - XRD of metakaolin-based mortars.

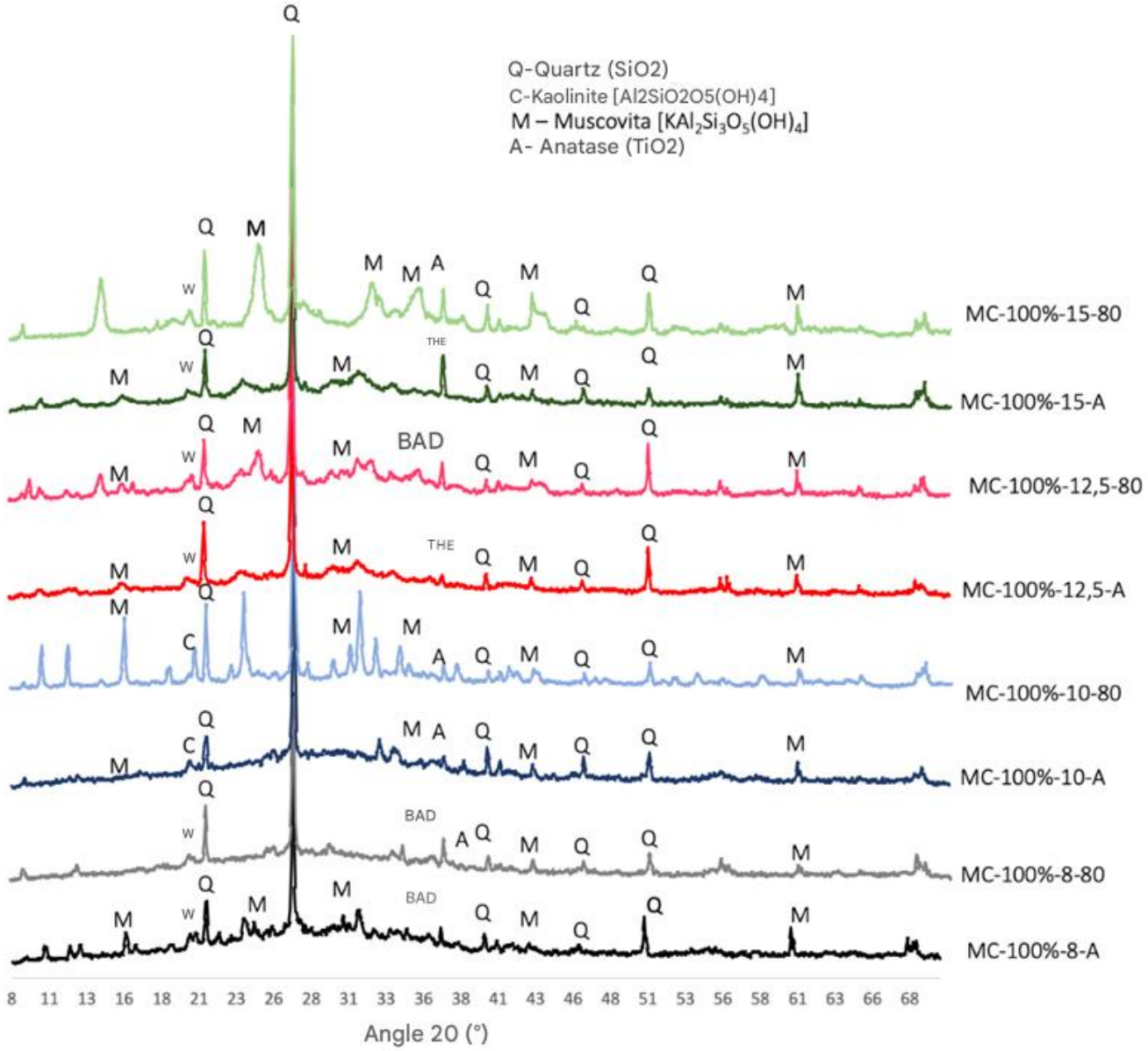

Figure 15 shows the XRD analyses of mortars with RTM as a precursor. It is noted that the number of samples tested was not the same as that of the other analytical techniques, since this test requires the sample to be distorted and placed in a metal sample holder in the form of dry powder. However, the samples with higher molar concentrations behaved plastically, not allowing the preparation. The alternative would be to dry in an oven, but due to the thermoactive nature of these alkali-activated materials, the results may not represent reality. Thus, only the RTM-100%-6-80, RTM-100%-8-80 and RTM-100%-10-80 samples were analyzed.

As previously described, RTM has a crystalline nature and the beneficiation process was not sufficient to create a raw material with good reactivity. Thus, only a small portion of amorphous material reacted with the alkaline activating solution, so that most of the peaks

Systematic Scientific Journal
ISSN: 2675-521

found in the analysis of RTM *in natura* (Figure 1) could also be observed in the final product. In fact, there was the formation of a matrix of the N-A-S-H type, since there are characteristics of a solid body with mechanical resistance.

It is concluded that the precursor was not completely dissolved due to the low compressive strengths obtained and leaching, found in the capillary absorption assay.

It can be seen, from the analysis of Figure 15, that the intensity of the peaks, at most angles, decreases for smaller molarities. It is noteworthy that it was in the lowest molarity (6 mol/liter) that the highest mechanical resistance was achieved. Thus, the increase in axial compressive strength is directly related to the intensity of the crystalline peaks and, consequently, to the formation of N-A-S-H.

Figure 15 - XRD of RTM-based mortars

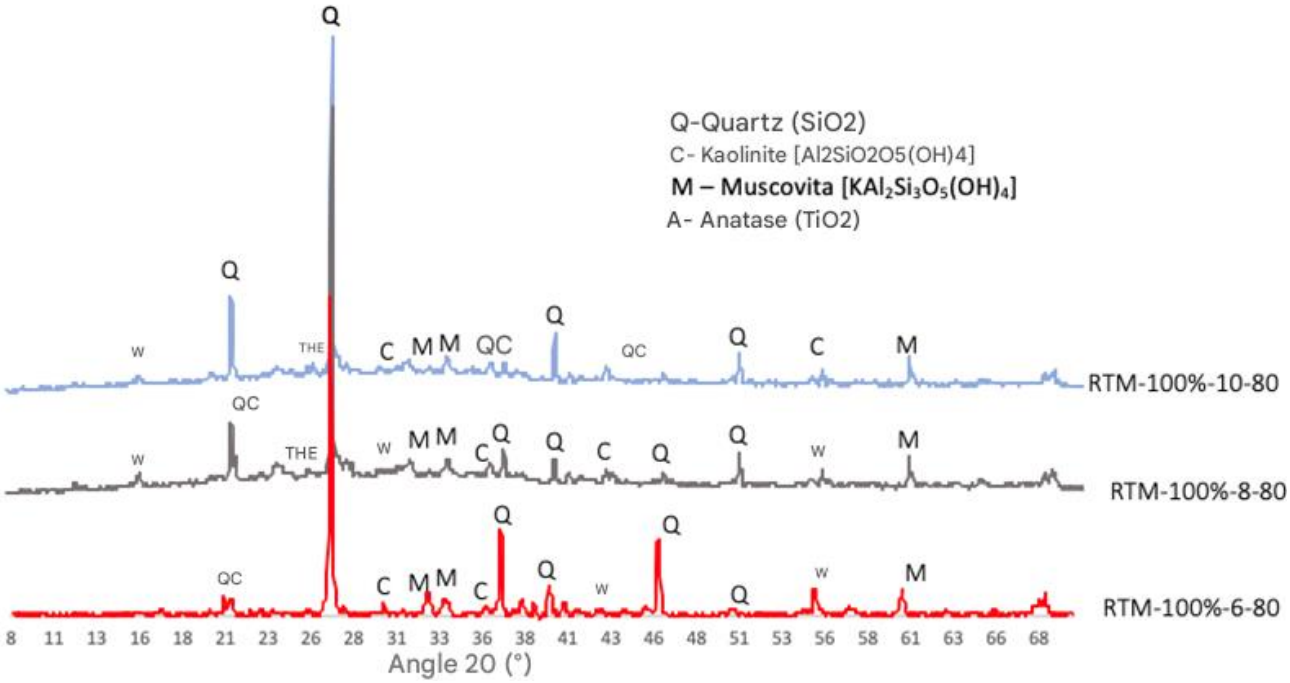

CONCLUSIONS

A total of 45 mortars were produced, varying the precursor (MC-100%, RTM-100% and MC+RTM-50%), the curing temperature (ambient, 60°C and 80°C) and the molarity of the alkaline activators (6, 8, 10, 12.5 and 15 mol/liter). From the analysis of the physical, chemical and mechanical results it was possible to conclude:

- the gain in axial compressive strength of the RTM mortars was in the direction of the lowest molarities; those with CM went in the opposite direction, up to 12.5 mol/liter;
- An 86.5-fold difference in axial compressive strength between MC-100%-12.5-80

Systematic Scientific Journal
ISSN: 2675-521

and RTM-100%-12.5-60 mortars was identified at the molar concentration of the alkaline activator of 12.5 mol/liter. This order of magnitude shows the superiority of metakaolin as a precursor when compared to RTM in terms of the formation of N-A-S-H (dense and resistant phase);

- the formation of efflorescence was identified in 100% of the mortars, which is a relevant pathology when dealing with alkali-activated materials;
- the lowest coefficients of water absorption by capillarity were observed at higher molarities for MC mortars;
- mortars with RTM suffered mass loss by leaching when in contact with water. This characteristic is associated with the low mechanical performance and crystallinity of the precursor. This behavior made the water absorption test by capillarity in these mortars unfeasible;
- the heat release corroborated the results of axial compressive strength, i.e., the pastes with higher strengths released more heat;
- in mortars with RTM, the low axial compressive strength, the low heat of reaction, together with the XRD results indicated high crystallinity of this precursor;
- Regarding applicability, the most viable mortar was MC-100%-12.5-60, as it did not present a significant difference from MC-100%-12.5-80. It is worth mentioning that, by varying the molarity of the alkaline activator solutions, there are significant gains in axial compressive strength without the use of thermal curing (gain of 17.5 MPa of the MC-100%-10-A mortar in relation to the MC-100%-12.5-A mortar);
- regarding capillary absorption, the most viable mortar was MC-100%-15-A, which did not differ significantly from MC-100%-15-80.

ACKNOWLEDGMENTS

This work was funded by the Universidade Estadual Norte Fluminense Darcy Ribeiro (UENF), in the Graduate Program in Civil Engineering (PPGEC), and by the Carlos Chagas Filho Foundation for Research Support of the State of Rio de Janeiro (FAPERJ).

Systematic Scientific Journal
ISSN: 2675-521

REFERENCES

1. T. Jiang, Z. Liu, X. Tian, J. Wu, L. Wang, Review on the impact of metakaolin-based geopolymer's reaction chemistry, nanostructure and factors on its properties, Construction and Building Materials, 412 (2024).

2. Z. Gao, Y. Li, H. Qian, M. Wei, Environmental, economic, and social sustainability assessment: a case of using contaminated tailings stabilized by waste-based geopolymer as road base, Sci. Total Environ, 888 (2023).

3. Q. Munir, M. Abdulkareem, M. Horttanainen, T. Karki, A comparative cradle-to-gate life cycle assessment of geopolymer concrete produced from industrial side streams in comparison with traditional concrete. Sci. Total Environ, 865 (2023).

4. M. Gómez-Casero, L. Pérez-Villarejo, E. Castro, D. Eliche-Quesada, Reinforcement of alkali-activated cements based matrices using olive pruning fibres as an alternative to traditional fibres, Sustainable Chemistry and Pharmacy, 37 (2024).

5. J. Provis, J. Van Deventer, Geopolymers: Structures, Processing, Properties and Industrial Applications. 1. ed. Cambridge, London: Woodhead Publishing, 2009, pp 464

6. J. Davidovits, Geopolymer Chemistry and Properties. Anais da 1ª Conferência Internacional sobre Geopolímero, Compiegne, v. 1, p. 25-48, (1988).

7. P. V. Krivenko, G.Y. Kovalchuk, Directed synthesis of alkaline aluminosilicate minerals in a geocement matrix. J. Mater. Sci., 42:2944-2952, (2007).

8. F. Pacheco-Torgal, J. Labrincha, C. Leonelli, A. Palomo, Handbook of alkali-activated cements, mortars and concretes. 1. ed. Cambridge, London: Woodhead Publishing, 830p, (2014).

9. J. Davidovits, Geopolymers - Inorganic polymeric new materials. Journal of Thermal Analysis 37(8): 1633-1656, (1991).

10. J. Davidovits, Properties of Geopolymeric Cements. Proceedings of the First International Conference on Alkaline Cements and Concretes. Kiev, Ukraine, v. 1, p. 131-149, (1994).

A. Fernández-Jiménez, A. Palomo, New Cementitious Materials Based on Alkali-Activated Fly Ash: Performance at High Temperatures. J. Am. Ceram. Soc., 91:3308-3314, (2008).

11. P Duxson, The structure and thermal evolution of metakaolin geopolymers. Tese de PhD, Universidade de Melbourne, Melbourne, Austrália, 2006.

12. F.L. Murta, Produção de argamassas a partir da ativação alcalina de metacaulim e de resíduo de tijolo moído por cales virgem e hidratada. Dissertação de MSc, UENF, Campos dos Goytacazes, RJ, 2008.

Systematic Scientific Journal
ISSN: 2675-521

13. J.C. Soares, Avaliação das propriedades físicas, mecânicas e características microestruturais de resinas geopoliméricas para recuperação de estruturas de concreto. Tese de DSc, UENF, Campos dos Goytacazes, RJ, 2020.

14. B. Sabir, S. Wild, J. Bai, Metakaolin and calcined clays as pozzolans for concrete: a review, Cem. Concr. Compos. 23 (2001).

15. ASSOCIAÇÃO BRASILEIRA DE NORMAS TÉCNICAS (2015) Areia normal para ensaio de cimento - Especificação: NBR 7214. Rio de Janeiro.

16. Associação Brasileira de Normas Técnicas (ABNT), Cimento Portland – Determinação da resistência à compressão. NBR 7215. Rio de Janeiro, 1996.

17. Associação Brasileira de Normas Técnicas (ABNT), Argamassa para assentamento e revestimento de paredes e tetos - Determinação da absorção de água por capilaridade e do coeficiente de capilaridade: NBR 15259. Rio de Janeiro, 2005.

18. Associação Brasileira de Normas Técnicas (ABNT), Argamassa para assentamento e revestimento de paredes e tetos – Preparo da mistura e determinação do índice de consistência: NBR 13276. Rio de Janeiro, 2016.

19. D.P. Dias, F.A. Silva, Effect of Na_2O/SiO_2 and K_2O/SiO_2 mass ratios on the compressive strength of non-silicate metakaolin geopolymeric mortars. Materials Research Express. MRX-113803.R1, (2019).

20. P. Duxson, J.L. Provis, LUKEY G.C., VAN DEVENTER J.S.J. 39K NMR of free potassium in geopolymers. Industrial & Engineering Chemistry Research, 45: 9208-9210, (2006).

21. M.A. Longhi, B. Walkley, E.D. Rodríguez, A.P. Kirchheim, Z. Zhang, H. Wang, New selective dissolution process to quantify reaction extent and product stability in metakaolin-based geopolymers. Composites Part B: Engineering. 176: 107172, (2019).

22. J.W. Tukey, Comparing Individual Means in the Analysis of Variance. Biometrics, 5:99-114, (1949).

23. C. Shi, A. Fernández-Jiménez, A. Palomo, New cements for the 21st century: The pursuit of an alternative to Portland cement. Cement and Concrete Research, 41:750-763, (2011).

24. LONGHI M.A., RODRÍGUEZ E. D., WALKLEY B., ZHANG Z., KIRCHHEIM A. P. Metakaolin-based geopolymers: Relation between formulation, physicochemical properties and efflorescence formation. Composites Part B: Engineering. 182: 107671, (2020).

25. N.T. Pandini, Influência da Relação Mássica CaO/SiO_2 nas Propriedades Tecnológicas de Argamassas à base de Cinza Volante Álcali-ativada com Cal Virgem. Dissertação de MSc, UENF, Campos dos Goytacazes, RJ, Brasil, 2019.

Systematic Scientific Journal
ISSN: 2675-521

26. M. Marvila, J. Alexandre, A.A.G. Rangel, E. Zanelato, S.N. Monteiro, G. Delaqua, L. Amaral, Estudo da Capilaridade para Argamassas de Múltiplo uso. Anais do Congresso Anual da ABM, v. 72, n. 1, (2017).

27. Associação Brasileira de Normas Técnicas (ABNT), Argamassa para assentamento e revestimento de paredes e tetos - Requisitos: NBR 13281. Rio de Janeiro, 2005.

28. H.S. Gonçalves, Argamassa de cinza volante álcali-ativada com resíduo da indústria de papel e celulose (Dregs, Grits e Lama de Cal. Dissertação de MSc, UENF, Campos dos Goytacazes, RJ, Brasil, 2021.

29. G. Macioski, Estudo da Álcali-ativação de Pó de Blocos Cerâmicos com Cal Hidratada. Dissertação de MSc , UTFPR, Curitiba, PR, Brasil, 2017.

30. Y. Cui, D. Wang, Y. Wang, R. Sun, Y. Rui, Effects of the n(H2O: Na_2Oeq) ratio on the geopolymerization process and T microstructures of fly ash-based geopolymers. Journal of Non-Crystalline Solids. 511:19-28, (2019).

31. W. Li, P.N. Lemougna, K. Wang, Y. He, Z. Tong, X. Cui, Effect of vacuum dehydration on gel structure and properties of metakaolin-based geopolymers. Ceramics International. 43: 14360-14-246, (2017).

32. S. Riahi, A. Nemati, A.R. Khodabandeh, S. Baghshahi, The effect of mixing molar ratios and sand particles on microstructure and mechanical properties of metakaolin-based geopolymers. Materials Chemistry and Physics. 240:122223 (2020).

33. S.O. Sore, A. Messan, E. Prud'Homme, G. Escadeillas, F. Tsobnang, Synthesis and characterization of geopolymer binders based on local materials from Burkina Faso – Metakaolin and rice husk ash. Construction and Building Materials 124 (2016) 301–311 (2016).

34. X. Lv, Y. Qin, Z. Lin, T. Tian, X. Cui. Inhibition of Efflorescence in Na-Based Geopolymer Inorganic Coating. ACS Omega. 5(24):14822-14830, (2020).

35. T.S. Rocha, D.P. Dias, F.C.C. França, R.R.S. Guerra, L.R.C.O Marques, Metakaolin-based geopolymer mortars with different alkaline activators (Na+ and K+). Construction and Building Materials, 1784:53–461, (2018).